PHYSICAL REVIEW D **95,** 033002 (2017)

Connecting the leptonic unitarity triangle to neutrino oscillation with *CP* violation in the vacuum and in matter

Hong-Jian He[1,2,*] and Xun-Jie Xu[1,†]

[1]*Institute of Modern Physics and Center for High Energy Physics, Tsinghua University, Beijing 100084, China*

[2]*Center for High Energy Physics, Peking University, Beijing 100871, China*

(Received 28 June 2016; published 14 February 2017)

Leptonic unitarity triangles (LUT) provide fundamental means to geometrically describe *CP* violation in neutrino oscillation. In this work, we use LUT to present a new geometrical interpretation of the vacuum oscillation probability and derive a compact new oscillation formula in terms of only three independent parameters of the corresponding LUT. Then, we systematically study matter effects in the geometrical formulation of neutrino oscillation with *CP* violation. Including nontrivial matter effects, we derive a very compact new oscillation formula by using the LUT formulation. We further demonstrate that this geometrical formula holds well for applications to neutrino oscillations in matter, including the long baseline experiments T2K, MINOS, NOν*A*, and DUNE.

DOI: 10.1103/PhysRevD.95.033002

I. INTRODUCTION

Discovering leptonic *CP* violation poses a major challenge to particle physics today and may uncover the origin of matter-antimatter asymmetry in the Universe [1]. Unitarity triangles provide the unique geometrical description of *CP* violations via 3×3 unitary matrix. They have played a vital role for studying *CP* violation of Cabibbo-Kobayashi-Maskawa (CKM) mixings in the quark sector [2]. So far, various neutrino oscillation experiments have been trying to precisely measure Pontecorvo-Maki-Nakagawa-Sakata (PMNS) mixings for the lepton-neutrino sector [3]. Leptonic unitarity triangles (LUT) provide a fundamental means to probe the leptonic *CP* violation, complementary to the usual method of measuring the *CP* asymmetry of neutrino oscillations, $P[\nu_\ell \to \nu_{\ell'}] - P[\bar{\nu}_\ell \to \bar{\nu}_{\ell'}]$ $(\ell \neq \ell')$ [4,5]. Some LUT studies appeared in the recent literature [6–9].

In Ref. [6], we found that LUT is directly connected to neutrino oscillations in vacuum. We proved [6] that the LUT angles exactly act as the *CP*-phase shifts of neutrino oscillations. We proved [6] that vacuum oscillation only depends on three independent geometrical parameters of the corresponding LUT. Because matter effects [10,11] in many current and future long baseline (LBL) oscillation experiments (such as T2K [12], MINOS [13], NOν*A* [14], and DUNE [15]) are non-negligible, it is important to develop our geometrical LUT formulation for including nontrivial matter effects.

In this work, we construct a new unified geometrical LUT formulation for neutrino oscillations in vacuum and in matter and study its applications. In Sec. II, we present a new geometrical LUT formulation to dynamically describe how a 3-neutrino system oscillates in vacuum. From this, we derive a new compact oscillation formula, manifestly in terms of only three independent parameters of the corresponding LUT. In Sec. III, we systematically study the LUT formulation for neutrino oscillations in matter. We derive an approximate analytical LUT formula including matter effects and further analyze its accuracy for the current and future long baseline oscillation experiments, in Sec. IV and Appendixes A and B. Finally, we conclude in Sec. V.

II. GEOMETRICAL FORMULATION OF NEUTRINO OSCILLATION IN VACUUM

From the unitarity of the PMNS matrix, $U^\dagger U = UU^\dagger = 1$, we have two sets of conditions, $\sum_j U_{\ell j} U^*_{\ell' j} = 0$ with $\ell \neq \ell'$ (forming the row triangles or "Dirac triangles") and $\sum_\ell U^*_{\ell j} U_{\ell j'} = 0$ with $j \neq j'$ (forming the column triangles or "Majorana triangles"). For the flavor neutrino oscillations, we consider the Dirac triangles $(\ell \neq \ell')$,

$$U_{\ell 1} U^*_{\ell' 1} + U_{\ell 2} U^*_{\ell' 2} + U_{\ell 3} U^*_{\ell' 3} = 0, \tag{1}$$

as shown in Fig. 1.

The sides and angles of each LUT (1) can be defined as follows,

$$(a, b, c) = (|U_{\ell 1} U^*_{\ell' 1}|, |U_{\ell 2} U^*_{\ell' 2}|, |U_{\ell 3} U^*_{\ell' 3}|), \tag{2a}$$

$$(\alpha, \beta, \gamma) = \arg\left(-\frac{U_{\ell 3} U^*_{\ell' 3}}{U_{\ell 2} U^*_{\ell' 2}}, -\frac{U_{\ell 1} U^*_{\ell' 1}}{U_{\ell 3} U^*_{\ell' 3}}, -\frac{U_{\ell 2} U^*_{\ell' 2}}{U_{\ell 1} U^*_{\ell' 1}}\right). \tag{2b}$$

*hjhe@tsinghua.edu.cn
†xunjie.xu@gmail.com

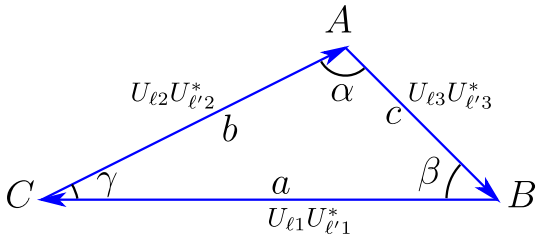

FIG. 1. The leptonic unitarity triangle (LUT), where $\ell \neq \ell'$, (a, b, c) denote lengths of the three sides, and (α, β, γ) represent the three angles.

In Ref. [6], we proved that the conventional neutrino oscillation probability in vacuum [4,5] can be fully expressed in terms of the sides (a, b, c) and angles (α, β, γ) of the corresponding LUT, among which only three are independent.

In the following, we propose a new geometrical approach. With this, we derive a new formula of vacuum oscillations, which manifestly contains only three independent parameters of the LUT for each given channel, say (b, c, α), and takes a very compact form.

In the standard formulation, the neutrino oscillation in space may be described by the following Schrödinger-like evolution equation in flavor basis,

$$\mathrm{i}\frac{\mathrm{d}}{\mathrm{d}L}|\nu(L)\rangle = H|\nu(L)\rangle, \tag{3}$$

where H is the effective Hamiltonian and $|\nu(L)\rangle$ denotes the flavor state of the flying neutrino at a distance L from the source. In vacuum, we can write the effective Hamiltonian H_0 in the following matrix form,

$$H_0 = \frac{1}{2E} U \begin{pmatrix} m_1^2 & & \\ & m_2^2 & \\ & & m_3^2 \end{pmatrix} U^\dagger. \tag{4}$$

Solving Eq. (3) gives $|\nu(L)\rangle = e^{-\mathrm{i}H_0 L}|\nu(0)\rangle$. So, the transition amplitude of $\nu_\ell \to \nu_{\ell'}$ takes the form, $A_{\ell\to\ell'} = \sum_j U_{\ell j} U^*_{\ell' j} e^{\mathrm{i}2\Delta_j}$, where $\Delta_j \equiv m_j^2 L/(4E)$. Thus, we deduce the oscillation probability $P_{\ell\to\ell'} = |A_{\ell\to\ell'}|^2$ as

$$\begin{aligned} P_{\ell\to\ell'} &= |U_{\ell 1}U^*_{\ell' 1}e^{\mathrm{i}2\Delta_1} + U_{\ell 2}U^*_{\ell' 2}e^{\mathrm{i}2\Delta_2} + U_{\ell 3}U^*_{\ell' 3}e^{\mathrm{i}2\Delta_3}|^2 \\ &= |a + be^{\mathrm{i}(\gamma-\pi)}e^{\mathrm{i}2\Delta_{21}} + ce^{\mathrm{i}(\pi-\beta)}e^{\mathrm{i}2\Delta_{31}}|^2, \end{aligned} \tag{5}$$

where in the second row we have used Eq. (2), and $\Delta_{jk} \equiv \Delta m_{jk}^2 L/(4E)$ with $\Delta m_{jk}^2 = m_j^2 - m_k^2$ $(j, k = 1, 2, 3)$.

We inspect Eq. (5) and find a new way to demonstrate its geometry graphically. For $L/E = 0$, we have $P_{\ell\to\ell'} = 0$ and $\Delta_{21} = \Delta_{31} = 0$. Hence, under $L/E = 0$, Eq. (5) reduces to

$$a + be^{\mathrm{i}(\gamma-\pi)} + ce^{\mathrm{i}(\pi-\beta)} = 0. \tag{6}$$

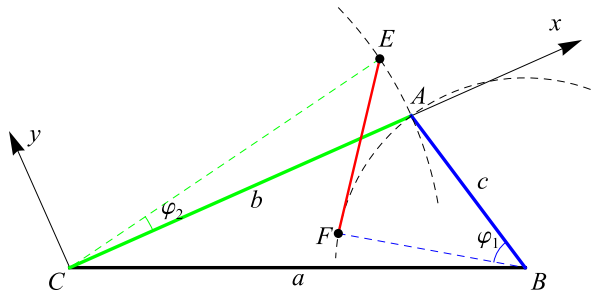

FIG. 2. New geometrical presentation of neutrino oscillation, where the angles $\angle ABF = \varphi_1$ and $\angle ACE = \varphi_2$ are evolving phases $\varphi_1 = L\Delta m_{31}^2/(2E)$ and $\varphi_2 = L\Delta m_{21}^2/(2E)$ in Eq. (7). The squared-distance $|EF|^2$ just gives the oscillation probability (5) via Eqs. (9) and (12). If the triangle is closed, $|EF| = 0$ and the probability vanishes. When L increases, point E and point F will circle around the corresponding dashed arcs, and the distance $|EF|$ oscillates. This means that the transition probability oscillates.

This just corresponds to the geometry of the LUT $\triangle ABC$ shown in Fig. 1. We re-present this picture in Fig. 2, where we have $(|BC|, |CA|, |AB|) = (a, b, c)$, and $(\angle CAB, \angle ABC, \angle BCA) = (\alpha, \beta, \gamma)$. We see that the triangle geometry $\overrightarrow{BC} + \overrightarrow{CA} + \overrightarrow{AB} = 0$ just gives the equality (6).

The generical case of $L/E \neq 0$ has nonzero oscillation factors $e^{\mathrm{i}2\Delta_{21}}$ and $e^{\mathrm{i}2\Delta_{31}}$. This will modify the equality (6), in which $e^{\mathrm{i}(\gamma-\pi)}$ is replaced by $e^{\mathrm{i}(\gamma-\pi)}e^{\mathrm{i}2\Delta_{21}}$ and $e^{\mathrm{i}(\pi-\beta)}$ by $e^{\mathrm{i}(\pi-\beta)}e^{\mathrm{i}2\Delta_{31}}$, causing nonzero probability (5). Geometrically, the phase factors $e^{\mathrm{i}2\Delta_{21}}$ and $e^{\mathrm{i}2\Delta_{31}}$ will change orientations of vectors $\overrightarrow{CA}$ and $\overrightarrow{BA}$ by holding their lengths. This will rotate $\overrightarrow{CA}$ to $\overrightarrow{CE}$ and $\overrightarrow{BA}$ to $\overrightarrow{BF}$, both counterclockwise. Denoting the angles $\angle ABF = \varphi_1$ and $\angle ACE = \varphi_2$, we have the following relations,

$$\varphi_1 = 2\Delta_{31}, \qquad \varphi_2 = 2\Delta_{21}. \tag{7}$$

This shows that the triangle is unfolded to become a quadrangle $ECBF$, and the side EF just equals the amplitude,

$$\overrightarrow{EF} = a + be^{\mathrm{i}(\gamma-\pi)}e^{\mathrm{i}2\Delta_{21}} + ce^{\mathrm{i}(\pi-\beta)}e^{\mathrm{i}2\Delta_{31}}. \tag{8}$$

Comparing this with Eq. (5), we conclude that

$$|EF|^2 = P_{\ell\to\ell'}, \tag{9}$$

just gives the oscillation probability. When the quadrangle $ECBF$ reduces to a closed triangle $\triangle ABC$, the oscillation probability would vanish. When L/E increases, point E and point F in Fig. 2 will circle around the corresponding dashed arcs. Thus, the distance $|EF|$ oscillates, and its square $|EF|^2$ exactly equals the oscillation probability (5) via Eq. (9). Hence, we have demonstrated that Fig. 2 and Eq. (9) give a new geometrical presentation of neutrino oscillations in vacuum.

We can directly compute the oscillation probability by using the above geometrical formulation. As shown below, it is striking that by using this geometrical formulation we can derive a very compact new formula of neutrino oscillations, manifestly in terms of only three LUT parameters. Without losing generality, we assign $\overrightarrow{CA}$ as the x-axis and its orthogonal direction as the y-axis. Thus, we can derive the following coordinates for points E and F in the x-y plane,

$$E:\ (b\cos\varphi_2, b\sin\varphi_2),$$
$$F:\ (b-2c\sin\frac{\varphi_1}{2}\cos\angle FAC,\quad -2c\sin\frac{\varphi_1}{2}\sin\angle FAC), \tag{10}$$

where the angle $\angle FAC=\alpha+\frac{1}{2}(\varphi_1-\pi)$. With these, we compute the length of the line segment EF as

$$|EF|^2 = 4c^2\sin^2\frac{\varphi_1}{2}+4b^2\sin^2\frac{\varphi_2}{2} - 8bc\sin\frac{\varphi_1}{2}\sin\frac{\varphi_2}{2}\cos\left(\frac{\varphi_1-\varphi_2}{2}+\alpha\right). \tag{11}$$

Using Eqs. (7), (9), and (11), we derive an elegant and very compact new formula of vacuum oscillations,

$$P_{\ell\to\ell'} = 4c^2\sin^2\Delta - 8bc\sin\Delta\sin\epsilon\Delta\cos[(1-\epsilon)\Delta+\alpha] + 4b^2\sin^2\epsilon\Delta, \tag{12}$$

where we have defined

$$\Delta\equiv\Delta_{31}=\frac{\Delta m^2_{31}L}{4E},\qquad \epsilon\equiv\frac{\Delta_{21}}{\Delta_{31}}=\frac{\Delta m^2_{21}}{\Delta m^2_{31}}. \tag{13}$$

The antineutrino oscillation probability $P_{\overline{\ell}\to\overline{\ell}'}$ can be obtained from Eq. (12) under the replacement $\alpha\to-\alpha$. The new oscillation formula (12) invokes only three independent geometrical parameters (b,c,α) of the corresponding LUT, while the other three nonindependent parameters (a,β,γ) have been explicitly removed in Eq. (12). Furthermore, this explicitly proves that the four PMNS-parameters $(\theta_{13},\theta_{23},\theta_{12},\delta)$ could enter the oscillation probability (12), only via their three independent combinations in terms of the geometrical parameters of LUT, such as (b,c,α). Note that Eq. (12) makes no approximation. But it may be regarded as a Taylor expansion in terms of $\sin\epsilon\Delta$ or ϵ, which is small due to $\epsilon\approx0.03$ [16,17] and $\Delta\sim O(1)$ for all known accelerator oscillation experiments [12–15]. In Eq. (12), the first row is of $O(\epsilon^0)$, serving as the leading order (LO). The second and third rows, of $O(\epsilon^1)$ and $O(\epsilon^2)$, belong to the next-to-leading order (NLO) and next-to-next-to-leading order (NNLO), respectively. No other higher order terms exist because Eq. (12) is exact.

Using our new Eq. (12), we can rederive the oscillation CP asymmetry $A^{\ell\ell'}_{CP}=P_{\ell\to\ell'}-P_{\overline{\ell}\to\overline{\ell}'}$,

$$A^{\ell\ell'}_{CP} = 32S_\triangle\sin\Delta\sin\epsilon\Delta\sin(1-\epsilon)\Delta = 4J(\sin2\Delta_{21}+\sin2\Delta_{13}+\sin2\Delta_{32}), \tag{14}$$

where (Δ,ϵ) are defined in Eq. (13), and the Jarlskog invariant J [18] equals twice of the LUT area, $J=2S_\triangle=bc\sin\alpha$. The last line of Eq. (14) agrees to the conventional CP asymmetry formula [5].

As a final remark, we consider the conventional vacuum oscillation formula [4,5],

$$P_{\ell\to\ell'} = \sum_{j=1}^{3}|U_{\ell' j}U_{\ell j}|^2 + 2\sum_{j<k}|U_{\ell' j}U_{\ell j}U_{\ell k}U_{\ell' k}|\cos(2\Delta_{jk}\mp\phi_{\ell'\ell;jk}), \tag{15}$$

where the signs "$\mp$" correspond to $\nu_\ell(\overline{\nu}_\ell)$ oscillations. Equation (15) contains the CP phase angle [4,5], $\phi_{\ell'\ell;jk}\equiv\arg(U_{\ell' j}U^*_{\ell j}U_{\ell k}U^*_{\ell' k})$. As we proved in Ref. [6], each CP-phase shift $\phi_{\ell'\ell;jk}$ exactly equals the corresponding angle of the LUT (modulo π), i.e., $(\phi_{\ell'\ell;23},\phi_{\ell'\ell;31},\phi_{\ell'\ell;12})=(\alpha,\beta,\gamma)+\pi$, where the convention of each LUT angle (α,β,γ) in Eq. (2b) differs from that of [6] by a minus sign. With this, we derived the vacuum oscillation probability $P[\nu_\ell\to\nu_{\ell'}]$, fully in terms of the geometrical parameters of the corresponding LUT [6],

$$P_{\ell\to\ell'} = 4ab\sin(\Delta_{12}\mp\gamma)\sin\Delta_{12} + 4bc\sin(\Delta_{23}\mp\alpha)\sin\Delta_{23} + 4ca\sin(\Delta_{31}\mp\beta)\sin\Delta_{31}, \tag{16}$$

according to the current convention of Eq. (2). Although Eq. (16) contains all six parameters (a,b,c) and (α,β,γ) of the LUT, only three are independent. Hence, if we choose three of them, say (b,c,α), the remaining parameters (a,β,γ) can all be expressed in terms of (b,c,α),

$$a=\sqrt{b^2+c^2-2bc\cos\alpha},\qquad \beta=\pi-(\alpha+\gamma),\qquad \gamma=\arccos\left(\frac{a^2+b^2-c^2}{2ab}\right). \tag{17}$$

We could try to eliminate the nonindependent parameters (a,β,γ) by substituting Eq. (17) into Eq. (16). But the resultant form is very complicated and lengthy. Only after we obtain the new formula (12) by the current geometrical approach [Fig. 1 and Eq. (9)], we could use Eq. (12) as the final answer (guideline) and eventually reduce Eq. (16) to Eq. (12) after tedious derivations. Our new formula (12) is

important because extending it we can further successfully construct the LUT formulation of neutrino oscillations including nontrivial matter effects, as we present in Secs. III and IV.

III. NEUTRINO OSCILLATIONS IN MATTER AND EFFECTIVE LEPTONIC UNITARITY TRIANGLE

Including matter effects requires adding the following new term H_i into the effective Hamiltonian H which appears in the evolution equation (3),

$$H_i = \sqrt{2} G_F N_e \begin{pmatrix} 1 & & \\ & 0 & \\ & & 0 \end{pmatrix}, \tag{18}$$

where the electron density $N_e = (Z/A)\rho N_A$, with ρ the matter density, Z (A) the atomic number (atomic mass number), and N_A the Avogadro constant. Equation (18) is for neutrino oscillations in matter, and for antineutrino oscillations the matter term (18) flips sign [5]. Including this matter term (18), we need to solve Eq. (3) with H given by

$$H = H_0 + H_i. \tag{19}$$

For the current LBL experiments, neutrino beams only pass through the crust of the Earth. So N_e is well approximated as a constant. Thus, we derive the solution of Eq. (3), $|\nu(L)\rangle = e^{-iHL}|\nu(0)\rangle$. The Hamiltonian H_0 can be diagonalized by the PMNS matrix U, but H cannot, i.e., $U^\dagger H_0 U$ is diagonal, but $U^\dagger H U = U^\dagger H_0 U + U^\dagger H_i U$ is not. Hence, we need to rediagonalize H by an effective mixing matrix $U_m (\equiv U + \delta U)$, which results in the effective neutrino masses $\tilde{m}_i$. Thus, we have

$$H = \frac{1}{2E} U_m \begin{pmatrix} \tilde{m}_1^2 & & \\ & \tilde{m}_2^2 & \\ & & \tilde{m}_3^2 \end{pmatrix} U_m^\dagger. \tag{20}$$

From the effective mixing matrix U_m, we can construct the effective leptonic unitarity triangles (ELUT), in the same way as we did for analyzing the vacuum LUT in Sec. III. When neutrino energy E is very low, $H_0 \gg H_i$ and U_m is fairly close to U. Hence, in the limit $E \to 0$, the ELUT simply reduce to the corresponding LUT. When E increases, ELUT gradually deviates from LUT since U_m deviates from U. Thus, the forms of ELUT will vary under the change of neutrino energy E.

The oscillation formula in matter is obtained by just replacing the original LUT parameters, say (b, c, α), by the new ELUT parameters (b_m, c_m, α_m). We make the same replacements for effective neutrino masses in Eq. (20).

This means that the geometrical presentation of neutrino oscillations in Fig. 2 still holds after including the matter effects. The only difference is to replace the vacuum LUT by the ELUT in matter and the neutrino masses $m_{1,2,3}$ by $\tilde{m}_{1,2,3}$. When a neutrino propagates in matter and its distance L increases, Point E and Point F in Fig. 2 will circle around the corresponding arcs in the ELUT frame. Then, the distance $|EF|$ oscillates, and $|EF|^2$ gives the oscillation probability in matter. Hence, including matter effects into Eq. (12), we deduce the oscillation formula,

$$\begin{aligned} P_{\ell\to\ell'} = {} & 4c_m^2 \sin^2\Delta_m \\ & - 8 b_m c_m \sin\Delta_m \sin(\epsilon_m \Delta_m) \cos[(1-\epsilon_m)\Delta_m + \alpha_m] \\ & + 4 b_m^2 \sin^2(\epsilon_m \Delta_m), \end{aligned} \tag{21}$$

where parameters with subscripts "m" denote the corresponding effective parameters in matter. For instance, b_m is the b-side of the ELUT from U_m in Eq. (20). Here, (Δ_m, ϵ_m) are obtained from (Δ, ϵ) [cf. Eq. (13)] under the replacements $m_{1,2,3} \to \tilde{m}_{1,2,3}$ [cf. Eq. (20)].

Note that Eq. (21) is an exact formula, and so far, we have not made any approximation. When neutrino energies lie between the solar resonance and atmospheric resonance, 0.1 GeV $\lesssim E \lesssim$ 3 GeV [19], one has the matter density $\rho \simeq 2.6$ g/cm^3 [20] for the Earth's crust, and the averaged ratio $Z/A \simeq 1/2$, where Z and A are the atomic number and mass number, respectively. With these, we deduce the approximate relations after a nontrivial and lengthy derivation,

$$c_m \simeq \frac{c}{1-n_E}, \qquad b_m \simeq \frac{\epsilon b}{n_E}, \qquad \alpha_m \simeq \alpha \pm \pi, \tag{22a}$$

$$\epsilon_m \simeq \frac{-n_E}{1-n_E}, \qquad \Delta_m \simeq (1-n_E)\Delta, \tag{22b}$$

where n_E is defined as

$$n_E = 2\sqrt{2} G_F N_e E / \Delta m_{31}^2. \tag{22c}$$

For clarity, we present the nontrivial derivation of Eq. (22) in Appendix A. These are important relations connecting the ELUT parameters in matter to the corresponding LUT parameters in vacuum. They allow us to use the vacuum LUT parameters to directly compute the oscillation probability in matter. This makes our LUT formulation applicable to the current and future LBL oscillation experiments [12–15]. In the following Sec. IV and Appendix B, we perform numerical analysis to explicitly test the accuracy of the above matter formulas (21) and (22) and discuss their validity.

IV. APPLICATIONS: TESTING THE PRECISION OF GEOMETRICAL OSCILLATION FORMULA

So far, most of the LBL experiments measure neutrino appearance via the oscillation channel $\nu_\mu \to \nu_e$. Using

our general geometrical equation (21) together with the approximate relations (22a) and (22b), we derive the following analytical LUT formula for the appearance oscillation probability,

$$P_{\rm LUT}(\nu_\mu \to \nu_e) = \frac{4c^2}{(1-n_E)^2}\sin^2[(1-n_E)\Delta] + \frac{4\epsilon^2 b^2}{n_E^2}\sin^2(n_E\Delta) - \frac{8\epsilon bc\sin[(1-n_E)\Delta]\sin(n_E\Delta)\cos(\Delta+\alpha)}{n_E(1-n_E)}. \quad (23)$$

The antineutrino oscillation probability $P_{\rm LUT}(\overline{\nu}_\mu \to \overline{\nu}_e)$ is obtained from Eq. (23) under the replacement $(\alpha, n_E) \to (-\alpha, -n_E)$. We stress that the new formula (23) is fully expressed in terms of only three independent parameters (b, c, α) of the LUT and is manifestly rephasing invariant. We also note that the form of Eq. (23) holds for both neutrino mass orderings. For the normal mass ordering $(m_1 < m_2 \ll m_3)$, Δ and ϵ are positive, while for the inverted mass ordering $(m_2 > m_1 \gg m_3)$, they are both negative.

In the following, we analyze the accuracy of Eq. (23) for practical applications. We first compute the probability from Eq. (23) and compare it with the exact numerical result from solving the neutrino evolution equation (3). We present this comparison in Fig. 3(a) and 3(b) for the ongoing NOνA experiment with baseline $L = 810$ km. In plot (a), the red dashed curves depict the prediction $P_{\rm LUT}$ of our LUT formula (23), and the green curve stands for the exact numerical result $P_{\rm Exact}$. In Fig. 3(b), we further present the difference $\Delta P = P_{\rm LUT} - P_{\rm Exact}$ by the red dashed curve.

For the comparison in Fig. 3, we further examine the approximate formula used by the Particle Data Group (PDG) [5,19,21],

$$\begin{aligned} P_{\rm PDG}(\nu_\mu \to \nu_e) &= \frac{1}{(1-n_E)^2}\sin^2\theta_a \sin^2 2\theta_x \sin^2[(1-n_E)\Delta] \\ &- \frac{\epsilon}{n_E(1-n_E)}\sin 2\theta_s \sin 2\theta_a \sin 2\theta_x \cos\theta_x \sin\delta \\ &\times \sin\Delta \sin(n_E\Delta)\sin[(1-n_E)\Delta] \\ &+ \frac{\epsilon}{n_E(1-n_E)}\sin 2\theta_s \sin 2\theta_a \sin 2\theta_x \cos\theta_x \cos\delta \\ &\times \cos\Delta \sin(n_E\Delta)\sin[(1-n_E)\Delta] \\ &+ \frac{\epsilon^2}{n_E^2}\sin^2 2\theta_s \cos^2\theta_a \sin^2(n_E\Delta), \end{aligned} \quad (24)$$

where $(\theta_s, \theta_a, \theta_x) \equiv (\theta_{12}, \theta_{23}, \theta_{13})$ and δ is the CP angle. Equation (24) is widely adopted by LBL experiments for data analysis, including the recent work of T2K [20]. (Some other approximate formulas using the conventional PMNS parametrization appeared in the literature [22].) Equation (24) is much more complex than our LUT Eq. (23). For comparison, we plot the probability $P_{\rm PDG}$ by blue dashed curves in Fig. 3(a). We further depict the difference $\Delta P = P_{\rm PDG} - P_{\rm Exact}$ (blue dashed curve) in Fig. 3(b). For illustrating the applications of Eqs. (23) and (24) in Fig. 3, we have input central values of the current global fit [16] for neutrino parameters under the normal mass ordering. We have also made similar comparisons under the inverted mass ordering.

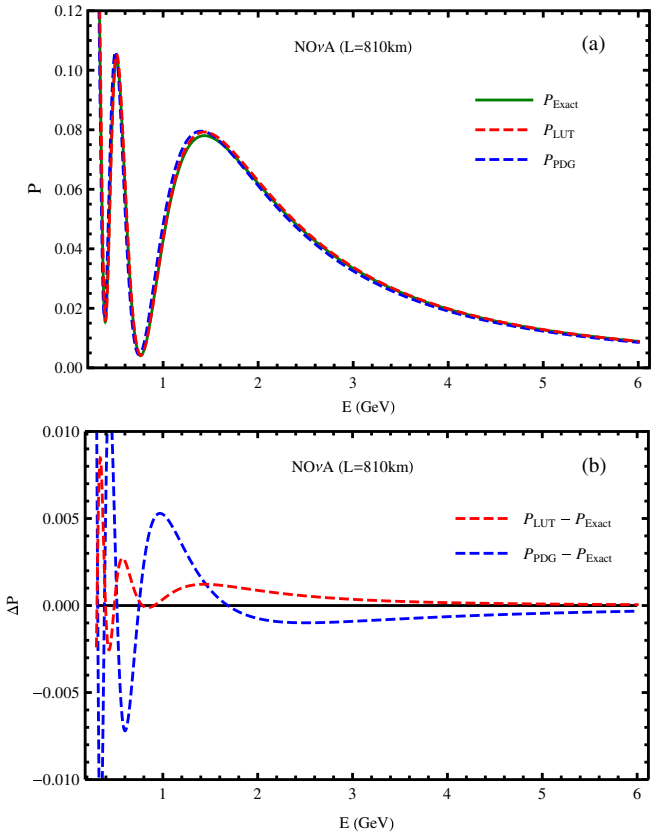

FIG. 3. Comparison of the approximate analytical oscillation formulas (23) and (24) with the exact numerical result (green curve) for the case of NOνA experiment ($L = 810$ km). Equation (23) is plotted in the red curve, and Eq. (24) is in blue curve. Plot (a) shows that both Eqs. (23) and (24) are fairly accurate, and their errors are negligible for practical use. Plot (b) depicts the differences $\Delta P = P_{\rm LUT} - P_{\rm Exact}$ (red curve) and $\Delta P = P_{\rm PDG} - P_{\rm Exact}$ (blue curve), showing that our LUT formula (23) is as accurate as (or better than) Eq. (24).

Figure 3 demonstrates that for applications to LBL experiments (such as NOνA [14]) our LUT formula (23) is very accurate, and its error is negligible for the current experimental precision. It shows that Eq. (23) is as precise as or better than the widely used PDG Eq. (24). Equation (23) contains only three independent LUT parameters (b, c, α) and is manifestly rephasing invariant. In contrast, Eq. (24) depends on all four PMNS-parameters $(\theta_s, \theta_a, \theta_x, \delta)$.

Note that Eq. (23) is derived from our independent new LUT approach and stands on its own, even though Fig. 3(a) shows that Eqs. (23) and (24) are in main agreement.

We stress that Eqs. (23) and (24) have their own advantages via two independent formulations of ν-oscillation; they are complementary for studying different aspects of neutrino oscillations. For current illustrations, we mainly consider the important on-going experiment NOνA ($L = 810$ km) [14] as an example. We have also reached similar conclusions by analyzing other LBL experiments MINOS ($L = 735$ km) [13] and T2K ($L = 295$ km) [20], as well as the planned future experiment DUNE ($L = 1300$ km) [15]. For further justifications of our LUT matter formula (23), we present explicit analyses for both T2K and DUNE experiments in Appendix B, covering a wide baseline range of $L = 295$–1300 km.

In passing, we note that, in principle, both formulas (23) and (24) require $\epsilon \ll n_E$, which corresponds to a lower bound on neutrino energy,

$$E \gtrsim 0.34\ \text{GeV}\left(\frac{\Delta m^2_{21}}{7.6\times 10^{-5}\ \text{eV}^2}\frac{1.4\ \text{cm}^{-3}N_A}{N_e}\right), \quad (25)$$

as given in Ref. [19] and updated by PDG [5] (cf. the note below Eq. (14.76) in Ref. [5]). For the NOνA experiment, the selected neutrino energy range is $1.5\ \text{GeV} \le E \le 2.7\ \text{GeV}$ [14], which well obeys the lower bound (25). For the case of the T2K experiment, it has a neutrino energy range of $0.1\ \text{GeV} \le E \le 1.2\ \text{GeV}$ [12]. So we may concern the validity of our formula for $E = (0.1$–$0.34)$ GeV. Our derivation in Sec. III has made the ϵ expansion, which requires $\epsilon \ll n_E$. We note that the approximate Eq. (22a) for b_m is singular in the limit $E \to 0$ (which causes $n_E \to 0$). But our Eq. (23) is free from this singularity because its $n_E = 0$ poles are actually canceled in the limit $n_E \to 0$. So, Eq. (23) still holds well around this limit. Also, a singularity $n_E = 1$ appears in Eq. (22a) for c_m. Again, it is fully canceled in Eq. (23) and is harmless. Note that the PDG Eq. (24) is also singularity-free in the limit $n_E \to 1$, or, $n_E \to 0$ [even though the perturbative expansion requires $\epsilon \ll n_E$ and thus the bound (25)]. But exact numerical calculations have verified that Eq. (24) remains fairly accurate below the bound (25). Hence, Eq. (24) was safely adopted by T2K analysis [12]. Reference [23] recently explained why Eq. (24) still holds at energies below the bound (25). For our LUT Eq. (23), we have demonstrated its validity for various oscillation experiments by comparing it with the exact numerical results in Fig. 3 and in Appendix B. We also expect similar reasons to explain the high numerical precision of our LUT Eq. (23) and will study the details of this issue elsewhere.

V. CONCLUSIONS

Leptonic unitarity triangles (LUT) provide fundamental means to geometrically describe CP violation in neutrino oscillations. In this work, we presented a new unified geometrical formulation for connecting the LUT to neutrino oscillations in vacuum and in matter. We demonstrated that the dependence of the vacuum oscillation probability on the PMNS mixing matrix can be reformulated in terms of only three independent geometrical parameters of the corresponding LUT, which are rephasing invariant. We further constructed the geometrical formulation of oscillations in matter and derived a very compact and accurate new oscillation formula.

In Sec. II, we proposed a new geometrical LUT formulation of the dynamical 3-neutrino oscillations. We proved that the vacuum oscillation probability can be derived by directly computing the distance of two points circling around a vertex of the LUT, as shown in Fig. 2 and given in Eqs. (9) and (12). Formula (12) manifestly depends on only three independent parameters of the corresponding LUT, and takes a much simpler form than Eqs. (16) and (17) which we derived before [6]. For neutrino oscillations in matter, we constructed the corresponding Effective LUT (ELUT) in Sec. III, which is a deformed LUT by including matter effects. Equations (21) and (22) presented a new geometrical oscillation formula including matter effects. Note that Eqs. (12) and (21) exhibit a LO + NLO + NNLO structure, but hold exactly without approximation. To analytically connect the ELUT parameters in Eq. (21) to the vacuum LUT parameters, we deduced new relations (22a) and (22b) under proper expansions, as shown in Appendix A. With these, we further derived a very compact analytical formula (23) in Sec. IV. We demonstrated that Eq. (23) has high accuracy for applications to long baseline experiments, such as NOνA (Fig. 3) and MINOS, as well as T2K and DUNE (cf. Figs. 4 and 5 in Appendix B). We showed that the numerical precision of our LUT formula (23) is as good as (or better than) the widely used PDG Eq. (24) [5], for the long baseline oscillation experiments T2K, MINOS, NOνA, and DUNE.

ACKNOWLEDGMENTS

We are grateful to Sheldon Glashow, John Ellis, Manfred Lindner, and Jose Valle for valuable discussions. We thank Eligio Lisi for useful discussions during and after his visit to Tsinghua HEP Center. We thank Yu-Chen Wang and Zhe Wang for useful discussions. This research was supported in part by the National Natural Science Foundation of China (under Grants No. 11275101, 11135003, 11675086) and by Tsinghua University (under Grant No. 20141081211).

APPENDIX A: DERIVATION OF MATTER FORMULA (22)

In this appendix, we present the highly nontrivial derivation of the matter formula (22), shown at the end of Sec. III in the main text.

Inspecting the effective Hamiltonian $H = H_0 + H_i$ in Eqs. (4) and (18), we can separate out a diagonal term $(m_1^2/2E)\mathbb{I}$ and express H as follows:

$$H = \frac{m_1^2}{2E}\mathbb{I} + \frac{\Delta m_{31}^2}{2E} U \mathbb{K} U^\dagger, \tag{A1}$$

where $\mathbb{I}$ is the 3×3 unit matrix. The dimensionless matrix $\mathbb{K}$ takes the following convenient form and needs to be diagonalized,

$$\mathbb{K} = \begin{pmatrix} 0 & & \\ & \epsilon & \\ & & 1 \end{pmatrix} + n_E u_e u_e^\dagger, \tag{A2}$$

where $u_e^\dagger$ is the first row of U. To be concrete, we parametrize U as

$$U = \begin{pmatrix} c_s c_x & s_s c_x & s_x \\ -e^{-\mathrm{i}\delta} s_s c_a - c_s s_a s_x & e^{-\mathrm{i}\delta} c_s c_a - s_s s_a s_x & s_a c_x \\ e^{-\mathrm{i}\delta} s_s s_a - c_s c_a s_x & -e^{-\mathrm{i}\delta} c_s s_a - s_s c_a s_x & c_a c_x \end{pmatrix}, \tag{A3}$$

where we have used notations, $(s_j, c_j) = (\sin\theta_j, \cos\theta_j)$ and $(\theta_s, \theta_a, \theta_x) = (\theta_{12}, \theta_{23}, \theta_{13})$. Thus, we have

$$u_e = (c_s c_x, s_s c_x, s_x)^T, \tag{A4}$$

where u_e is real under this convention, and thus $u_e^\dagger = u_e^T$. Hence, we are actually going to diagonalize a real matrix $\mathbb{K}$. The final result of computing the ELUT does not depend on the parametrization of U. Note that Eq. (A3) can be obtained from the standard parametrization of PMNS matrix U_S [5] via simple rephasing,

$$U = \mathrm{diag}(1, e^{-\mathrm{i}\delta}, e^{-\mathrm{i}\delta}) U_S \mathrm{diag}(1, 1, e^{\mathrm{i}\delta}), \tag{A5}$$

where U_S is given by [5],

$$U_S = \begin{pmatrix} c_s c_x & s_s c_x & e^{-\mathrm{i}\delta} s_x \\ -s_s c_a - e^{\mathrm{i}\delta} c_s s_a s_x & c_s c_a - e^{\mathrm{i}\delta} s_s s_a s_x & s_a c_x \\ s_s s_a - e^{\mathrm{i}\delta} c_s c_a s_x & -c_s s_a - e^{\mathrm{i}\delta} s_s c_a s_x & c_a c_x \end{pmatrix}. \tag{A6}$$

Using the following 1-2 rotation

$$O_{12} = \begin{pmatrix} c_s & -s_s & 0 \\ s_s & c_s & 0 \\ 0 & 0 & 1 \end{pmatrix}, \tag{A7}$$

we can rotate u_e into a vector containing only two nonzero elements,

$$u_e^\dagger O_{12} = u_e^T O_{12} = (c_x, 0, s_x). \tag{A8}$$

Then, we find that $n_E u_e u_e^\dagger$ in Eq. (A2) will be rotated into a matrix having only two off-diagonal elements,

$$n_E O_{12}^T (u_e u_e^\dagger) O_{12} = n_E \begin{pmatrix} c_x^2 & 0 & s_x c_x \\ 0 & 0 & 0 \\ s_x c_x & 0 & s_x^2 \end{pmatrix}. \tag{A9}$$

For $\epsilon = 0$, after the 1–2 rotation O_{12}, Eq. (A2) will be rotated to

$$O_{12}^T \mathbb{K}_0 O_{12} = \begin{pmatrix} 0 & & \\ & 0 & \\ & & 1 \end{pmatrix} + n_E \begin{pmatrix} c_x^2 & 0 & s_x c_x \\ 0 & 0 & 0 \\ s_x c_x & 0 & s_x^2 \end{pmatrix}, \tag{A10}$$

where $\mathbb{K}_0$ is defined as, $\mathbb{K}_0 = \mathbb{K}|_{\epsilon=0}$. Thus, to diagonalize the matrix in Eq. (A10), we just need a 1–3 rotation,

$$O_{13} = \begin{pmatrix} c_\theta & 0 & s_\theta \\ 0 & 1 & 0 \\ -s_\theta & 0 & c_\theta \end{pmatrix}, \tag{A11}$$

where $(s_\theta, c_\theta) = (\sin\theta, \cos\theta)$. Under the rotation (A11), Eq. (A8) is transformed to

$$u_e^\dagger O_{12} O_{13} = (c_y, 0, s_y), \tag{A12}$$

where $(s_y, c_y) = (\sin\theta_y, \cos\theta_y)$, and $\theta_y = \theta + \theta_x$. Then, the matrix (A10) is rotated to

$$\begin{aligned} O_{13}^T O_{12}^T \mathbb{K}_0 O_{12} O_{13} &= \begin{pmatrix} s_\theta^2 & 0 & -s_\theta c_\theta \\ 0 & 0 & 0 \\ -s_\theta c_\theta & 0 & c_\theta^2 \end{pmatrix} + n_E \begin{pmatrix} c_y^2 & 0 & s_y c_y \\ 0 & 0 & 0 \\ s_y c_y & 0 & s_y^2 \end{pmatrix} \\ &= \begin{pmatrix} \lambda_- & 0 & 0 \\ 0 & 0 & 0 \\ 0 & 0 & \lambda_+ \end{pmatrix}, \end{aligned} \tag{A13}$$

where we have defined

$$\lambda_- = s_\theta^2 + n_E c_y^2, \qquad \lambda_+ = c_\theta^2 + n_E s_y^2. \tag{A14}$$

In the second equality of Eq. (A13), we have imposed the following condition on the (1,3) and (3,1) elements to ensure full diagonalization,

$$n_E s_y c_y - s_\theta c_\theta = 0. \tag{A15}$$

This leads to

$$\sin(2\theta) = n_E \sin(2\theta_y). \tag{A16}$$

Given the relation $\theta_y = \theta + \theta_x$, we can solve θ as a function of θ_x,

$$\tan 2\theta = \frac{n_E \sin(2\theta_x)}{1 - n_E \cos(2\theta_x)}. \tag{A17}$$

Hence, we have determined the 1–3 rotation and diagonalized the matrix $\mathbb{K}$ under $\epsilon = 0$ limit. The diagonalization matrix is $O_{12}O_{13}$, and the effective mixing matrix in this case corresponds to $U_{m0} \equiv U_m|_{\epsilon=0}$, as given by

$$U_{m0} = UO_{12}O_{13} = \begin{pmatrix} c_y & 0 & s_y \\ -s_y s_a & c_a e^{-i\delta} & c_y s_a \\ -s_y c_a & -s_a e^{-i\delta} & c_y c_a \end{pmatrix}. \tag{A18}$$

Hence, when $\epsilon = 0$, the effective unitarity triangle extracted from Eq. (A18) is actually a line for $\nu_e - \nu_\mu$ or $\nu_e - \nu_\tau$ oscillations, since in either case the length of the b side vanishes,

$$b_{m0} = 0. \tag{A19}$$

The other two sides of this LUT have the same length,

$$a_{m0} = c_{m0} = \frac{c}{\sqrt{(1-n_E)^2 + 4n_E s_x^2}}, \tag{A20}$$

where $c = s_x c_x s_a$ (or $c = s_x c_x c_a$) is the length of c side of the vacuum LUT for $\nu_e - \nu_\mu$ (or, $\nu_e - \nu_\tau$) oscillations. We have made use of Eqs. (A16) and (A17) for deriving the formula (A20).

Next, we compute the corrections from nonzero ϵ. For $\epsilon \neq 0$, we can split the matrix $\mathbb{K}$ in Eq. (A2) as follows:

$$\mathbb{K} \equiv \mathbb{K}_0 + \mathbb{K}_\epsilon, \tag{A21}$$

where

$$\mathbb{K}_0 = \begin{pmatrix} 0 & & \\ & 0 & \\ & & 1 \end{pmatrix} + n_E u_e u_e^T, \qquad \mathbb{K}_\epsilon = \begin{pmatrix} 0 & & \\ & \epsilon & \\ & & 0 \end{pmatrix}. \tag{A22}$$

Then, under the rotation $O_{12}O_{13}$, the matrix $\mathbb{K}_\epsilon$ transforms as

$$O_{13}^T O_{12}^T \mathbb{K}_\epsilon O_{12}O_{13} = \epsilon \begin{pmatrix} s_s^2 & s_s c_s & 0 \\ s_s c_s & c_s^2 & 0 \\ 0 & 0 & 0 \end{pmatrix} + \mathcal{O}(10^{-3}), \tag{A23}$$

where the corrections due to O_{13} rotation are suppressed by $\epsilon\theta_{13} = \mathcal{O}(10^{-3})$ and are negligible in the final result. Hence, under the rotations $O_{12}O_{13}$, we have the matrix $\mathbb{K}$ transform as

$$\mathbb{K} \to \begin{pmatrix} \lambda_- & 0 & 0 \\ 0 & 0 & 0 \\ 0 & 0 & \lambda_+ \end{pmatrix} + \epsilon \begin{pmatrix} s_s^2 & s_s c_s & 0 \\ s_s c_s & c_s^2 & 0 \\ 0 & 0 & 0 \end{pmatrix} + \mathcal{O}(10^{-3}). \tag{A24}$$

We can further diagonalize the right-hand side of Eq. (A24) by a rotation O'_{12},

$$O'_{12} = \begin{pmatrix} c_r & -s_r & 0 \\ s_r & c_r & 0 \\ 0 & 0 & 1 \end{pmatrix}, \tag{A25}$$

where $(s_r, c_r) = (\sin\theta_r, \cos\theta_r)$. Thus, we can determine the angle θ_r as follows:

$$\tan 2\theta_r = \frac{\epsilon \sin(2\theta_s)}{\lambda_- - \epsilon\cos(2\theta_s)}. \tag{A26}$$

With these, we combine the above rotation O'_{12} with U_{m0} in Eq. (A18) and deduce the following rotation for full diagonalization:

$$U_m = U_{m0}O'_{12} = \begin{pmatrix} c_y c_r & -s_r c_y & s_y \\ s_r c_a e^{-i\delta} - c_r s_a s_y & c_r c_a e^{-i\delta} + s_r s_y s_a & c_y s_a \\ \times & \times & \times \end{pmatrix}, \tag{A27}$$

where $\times$ stands for the elements irrelevant to our current concern. For the $\nu_e - \nu_\mu$ LUT, using Eqs. (A27) and (A26), we derive

$$\begin{aligned} b_m &= s_r c_y |c_r c_a e^{-i\delta} + s_r s_y s_a| \\ &= \frac{\epsilon s_{2s} c_a c_y}{2\sqrt{(\lambda_- - \epsilon c_{2s})^2 + \epsilon^2 s_{2s}^2}}[1 + \mathcal{O}(\epsilon\theta_x)], \end{aligned} \tag{A28}$$

where $(s_{2s}, c_{2s}) = (\sin 2\theta_s, \cos 2\theta_s)$. This gives a small but nonzero length for the b-side of the deformed effective unitarity triangle,

$$b_m \simeq \frac{\epsilon}{\lambda_-} b. \tag{A29}$$

The length of c-side is not changed from the leading order result because the last column of U_m equals that of U_{m0},

$$c_m \simeq c_{m0}, \tag{A30}$$

with c_{m0} given by Eq. (A20). Since the current global fits of neutrino data [16,17] restrict the 3σ range of $\theta_{13} \equiv \theta_x \simeq 0.137$–$0.158 = \mathcal{O}(0.1) \ll 1$, we see that $s_y^2 \sim s_\theta^2 \sim s_x^2 = \mathcal{O}(10^{-2})$ are fairly small. This applies to Eqs. (A20) and (A14). Hence, we derive the approximate relations, $b_m \simeq \epsilon b/n_E$ and $c_m \simeq c/(1-n_E)$, which lead to Eq. (22a).

From the definition of α in Eq. (2b), and using the formulas (A3) and (A27), we have $\alpha = -\arg(-U_{\mu 2})$ and

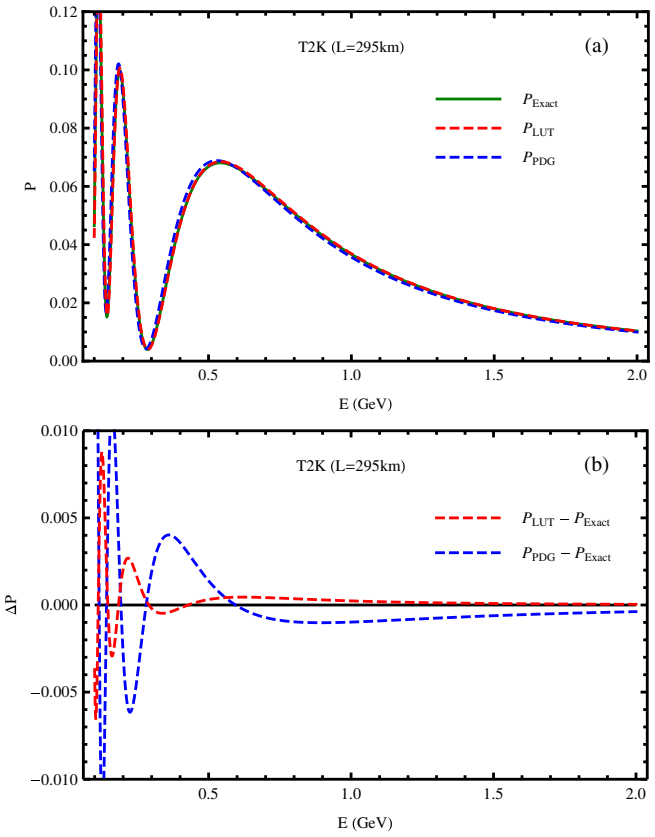

FIG. 4. Same as Fig. 3 in the main text, except changing the baseline length to $L = 295$ km, representing the case of T2K experiment. In plot (a), the green solid curve stands for the exact numerical result $P_{\rm Exact}$, the red dashed curve denotes the prediction $P_{\rm LUT}$ of the approximate analytical LUT formula (23), and the blue dashed curve depicts the result $P_{\rm PDG}$ of the approximate analytical PDG formula (24). Plot (b) depicts the differences $\Delta P = P_{\rm LUT} - P_{\rm Exact}$ (red curve) and $\Delta P = P_{\rm PDG} - P_{\rm Exact}$ (blue curve), showing that our LUT formula (23) is as accurate as (or better than) Eq. (24) for the case of T2K experiment.

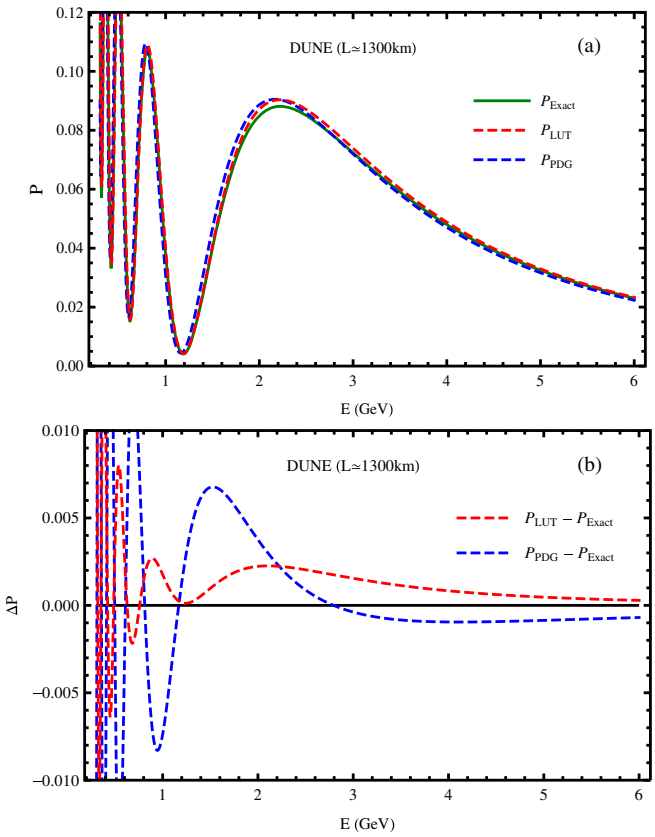

FIG. 5. Same as Fig. 3 in the main text, except changing the baseline length to $L = 1300$ km, representing the case of DUNE experiment. In plot (a), the green solid curve stands for the exact numerical result $P_{\rm Exact}$, the red dashed curve denotes the prediction $P_{\rm LUT}$ of the approximate analytical LUT formula (23), and the blue dashed curve depicts the result $P_{\rm PDG}$ of the approximate analytical PDG formula (24). Plot (b) depicts the differences $\Delta P = P_{\rm LUT} - P_{\rm Exact}$ (red curve) and $\Delta P = P_{\rm PDG} - P_{\rm Exact}$ (blue curve), showing that our LUT formula (23) is as accurate as (or better than) Eq. (24) for the case of DUNE experiment.

$\alpha_m = -\arg((U_m)_{\mu 2})$, where the expression of α_m does not have a "$-$" sign in front of $(U_m)_{\mu 2}$ because it is canceled by the negative sign in $(U_m)_{e2}$. Ignoring $s_x, s_y = \mathcal{O}(0.1)$, we have $\arg(U_{\mu 2}) \simeq \arg((U_m)_{\mu 2})$, and thus $\alpha_m \simeq \alpha \pm \pi$, which reproduces the third relation of Eq. (22a). Hence, the final ELUT is approximately given by Eq. (22a). To derive Eq. (22b), we note that at $\mathcal{O}(\epsilon^0)$ the eigenvalues of the matrix $\mathbb{K}$ in Eq. (A24) are $(\lambda_-, 0, \lambda_+)$. Accordingly, the effective Hamiltonian (A1) has three eigenvalues,

$$\left(\frac{m_1^2 + \Delta m_{31}^2 \lambda_-}{2E}, \frac{m_1^2}{2E}, \frac{m_1^2 + \Delta m_{31}^2 \lambda_+}{2E}\right), \tag{A31}$$

which should equal the corresponding eigenvalues $(\tilde{m}_1^2, \tilde{m}_2^2, \tilde{m}_3^2)/(2E)$ as defined in Eq. (20). Hence, we deduce the effective mass squared differences at $\mathcal{O}(\epsilon^0)$,

$$\begin{aligned} \Delta\tilde{m}_{31}^2 &\simeq (\lambda_+ - \lambda_-)\Delta m_{31}^2, \\ \Delta\tilde{m}_{21}^2 &\simeq (-\lambda_-)\Delta m_{31}^2. \end{aligned} \tag{A32}$$

Using this and Eq. (A14), we derive the approximate formulas, $\epsilon_m \simeq -n_E/(1-n_E)$ and $\Delta_m \simeq (1-n_E)\Delta$, by dropping small $\mathcal{O}(s_x^2)$ terms. This just reproduces Eq. (22b) in the main text.

In summary, we have proven the approximate formulas (22a) and (22b) in the main text.

APPENDIX B: FURTHER TESTS OF MATTER FORMULA (23)

In this appendix, we further present two important tests of our new LUT formula (23) by using the LBL oscillation experiments T2K [20] and DUNE [15].

The baselines of the T2K and DUNE experiments are $L = 295$ km and $L = 1300$ km, respectively. We present the predictions of our Eq. (23) for the T2K experiment in Fig. 4(a) and for DUNE experiment in Fig. 5(a), by the red dashed curves. Then, we compare them with the exact numerical results (green solid curves) in each plot. For comparison, we further show the results of the conventional formula (24) (used by the PDG [5]) in the blue dashed curves. We see that in each case the three curves agree with each other to high precision, similar to our findings in Fig. 3 for NOνA experiment. In Figs. 4(b) and 5(b), we further compare the differences, $\Delta P = P_{\rm LUT} - P$ (red dashed curves) and $\Delta P = P_{\rm PDG} - P$ (blue dashed curves). Again, these comparisons explicitly demonstrate that our LUT formula (23) is as accurate as (or better than) the conventional PDG formula (24).

[1] For a review, W. Buchmuller, R. D. Peccei, and T. Yanagida, Annu. Rev. Nucl. Part. Sci. **55**, 311 (2005) and references therein.

[2] N. Cabibbo, Phys. Rev. Lett. **10**, 531 (1963); M. Kobaya-shi and T. Maskawa, Prog. Theor. Phys. **49**, 652 (1973).

[3] B. Pontecorvo, Zh. Eksp. Teor. Fiz. **33**, 549 (1957) Sov. Phys. JETP **6**, 429 (1957); B. PontecorvoZh. Eksp. Teor. Fiz. **34**, 247 (1958) Sov. Phys. JETP **7**, 172 (1958); Z. Maki, M. Nakagawa, and S. Sakata, Prog. Theor. Phys. **28**, 870 (1962).

[4] For a review, S. M. Bilenky and S. T. Petcov, Rev. Mod. Phys. **59**, 671 (1987) and references therein.

[5] C. Patrignani *et al.* (Particle Data Group Collaboration), Chin. Phys. C **40**, 100001 (2016).

[6] H. J. He and X. J. Xu, Phys. Rev. D **89**, 073002 (2014).

[7] For examples, H. Fritzsch and Z. Z. Xing, Prog. Part. Nucl. Phys. **45**, 1 (2000); J. A. Aguilar-Saavedra and G. C. Branco, Phys. Rev. D **62**, 096009 (2000); J. Sato, Nucl. Instrum. Methods Phys. Res., Sect. A **472**, 434 (2001); Y. Farzan and A. Yu. Smirnov, Phys. Rev. D **65**, 113001 (2002); Y. Koide, arXiv:hep-ph/0502054; H. Zhang and Z. Z. Xing, Eur. Phys. J. C **41**, 143 (2005); S. Antusch, C. Biggio, E. Fernandez-Martinez, M. B. Gavela, and J. Lopez-Pavon, J. High Energy Phys. 10 (2006) 084; J. D. Bjorken, P. F. Harrison, and W. G. Scott, Phys. Rev. D **74**, 073012 (2006); G. Ahuja and M. Gupta, Phys. Rev. D **77**, 057301 (2008); A. Dueck, S. Petcov, and W. Rodejohann, Phys. Rev. D **82**, 013005 (2010); S. Luo, Phys. Rev. D **85**, 013006 (2012); P. S. B. Dev, C. H. Lee, and R. N. Mohapatra, Phys. Rev. D **88**, 093010 (2013); Z. Z. Xing and J. Y. Zhu, Nucl. Phys. **B908**, 302 (2016); J. High Energy Phys. 07 (2016) 011 and references therein.

[8] X. J. Xu, H. J. He, and W. Rodejohann, J. Cosmol. Astropart. Phys. 12 (2014) 039.

[9] H. J. He, W. Rodejohann, and X. J. Xu, Phys. Lett. B **751**, 586 (2015).

[10] L. Wolfenstein, Phys. Rev. D **17**, 2369 (1978).

[11] S. P. Mikheev and A. Yu. Smirnov, Sov. J. Nucl. Phys. **42**, 913 (1985); Nuovo Cimento C **9**, 17 (1986).

[12] K. Abe *et al.* (T2K Collaboration), Phys. Rev. Lett. **112**, 061802 (2014).

[13] P. Adamson *et al.* (MINOS Collaboration), Phys. Rev. Lett. **106**, 181801 (2011).

[14] P. Adamson *et al.* (NOνA Collaboration), Phys. Rev. Lett. **116**, 151806 (2016); D. S. Ayres *et al.* (NOνA Collaboration), arXiv:hep-ex/0503053.

[15] R. Acciarri *et al.* (DUNE Collaboration), arXiv:1512.06148.

[16] F. Capozzi, E. Lisi, A. Marrone, D. Montanino, and A. Palazzo, Nucl. Phys. **B908**, 218 (2016) and references therein.

[17] D. V. Forero, M. Tortola, and J. W. F. Valle, Phys. Rev. D **90**, 093006 (2014) and references therein.

[18] C. Jarlskog, Phys. Rev. Lett. **55**, 1039 (1985).

[19] M. Freund, Phys. Rev. D **64**, 053003 (2001).

[20] K. Abe *et al.* (T2K Collaboration), Phys. Rev. D **88**, 032002 (2013).

[21] A. Cervera, A. Donini, M. B. Gavela, J. J. G. Cadenas, P. Hernandez, O. Mena, and S. Rigolin, Nucl. Phys. **B579**, 17 (2000); **B593**, 731(E) (2001).

[22] For example, E. K. Akhmedov, P. Huber, M. Lindner, and T. Ohlsson, Nucl. Phys. **B608**, 394 (2001); P. F. Harrison and W. G. Scott, Phys. Lett. B **535**, 229 (2002); E. K. Akhmedov, R. Johansson, M. Lindner, T. Ohlsson, and T. Schwetz, J. High Energy Phys. 04 (2004) 078; A. Takamura, K. Kimura, and H. Yokomakura, Phys. Lett. B **595**, 414 (2004); S. K. Agarwalla, Y. Kao, and T. Takeuchi, J. High Energy Phys. 04 (2014) 047; O. Yasuda, Phys. Rev. D **89**, 093023 (2014) 093023 and references therein.

[23] X. J. Xu, J. High Energy Phys. 10 (2015) 090.